Supporting Information for Reconfigurable Holographic Patterns for Optical Security Multiplexing Fabricated by 3D Spatially Modulated Femtosecond Pulses

Peng Yi¹, Zhipeng Wang¹, Lan Jiang^{1,2,3*}, Xiaowei Li¹, Yang Liu⁴, Taoyong Li¹, Andong Wang¹, Zhi Wang¹, Xiangyu Zhang¹, Ji Huang^{1,5}, Qunshuo Wei⁶, and Jiafang Li⁷, Lingling Huang⁶

¹ Laser Micro/Nano Fabrication Laboratory, School of Mechanical Engineering, Beijing Institute of Technology, Beijing 100081, China

² Beijing Institute of Technology Chongqing Innovation Center, Chongqing, 401120, China

³Yangtze Delta Region Academy of Beijing Institute of Technology, Jiaxing, 314019, China

⁴ Institute of Micro-Nano Optoelectronics and Terahertz Technology, School of Mechanical Engineering, Jiangsu University, Zhenjiang 212013 PR China

⁵ National Institute of Metrology, Beijing 100029, China

⁶ School of Optics and Photonics, Beijing Institute of Technology, Beijing, 100081, China

⁷ Beijing Key Lab of Nanophotonics & Ultrafine Optoelectronic Systemsand School of PhysicsBeijing Institute of TechnologyBeijing 100081, China

1. Fabrication of a 3D multilayer pattern containing six layers of zone

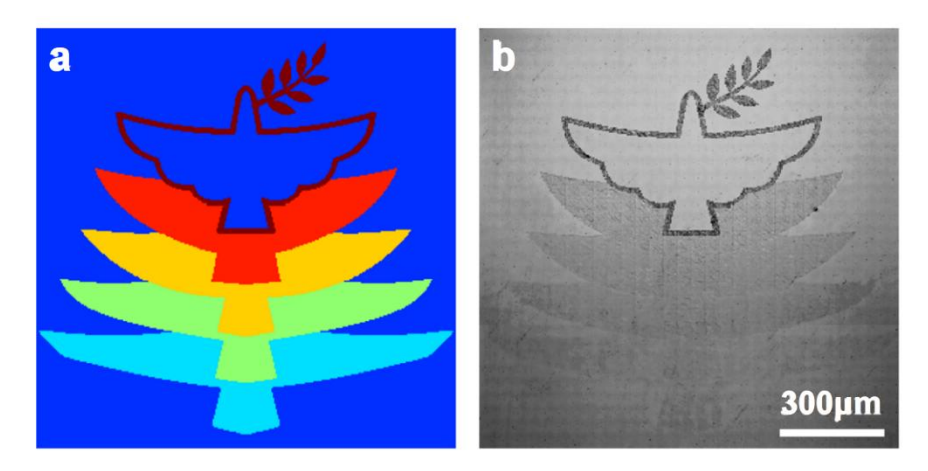


Figure S1. (a) The corresponding 2D pattern containing 6 zones depicted with different colors. (b) The complete optical microscope image of fabricated 3D multilayer pattern.

2. Optical systems for reconstruction of the holographic images and observation of the holographic patterns

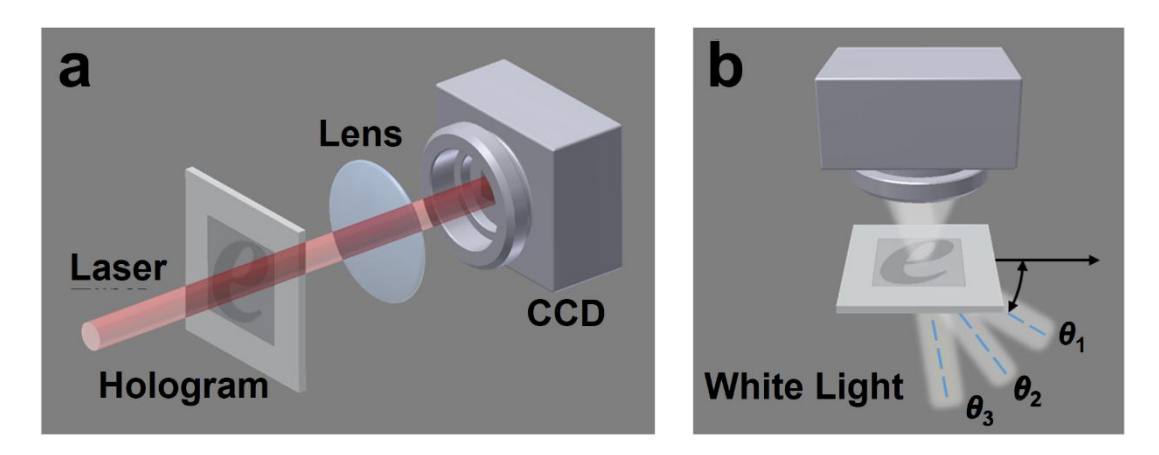


Figure S2. Scheme of the optical systems for (a) measuring the holographic images, in which a supercontinuum laser source was employed, and (b) capturing the photographs of holographic patterns observed under white light illumination of different angles.

3. Near-field images of the holographic pattern under coherent illumination

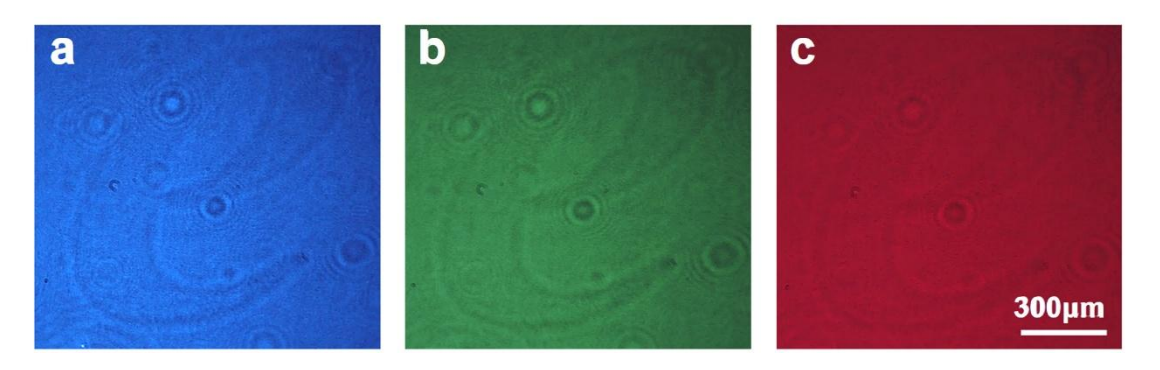


Figure S3. The near field images of holographic pattern magnified through an objective $(20\times, NA = 0.45)$ under the vertical irradiation of laser beams with wavelengths of (a) 470 nm, (b) 532 nm and (c) 633 nm.

4. Design of holographic pattern encoding two different images

Two images containing "1940" and "BIT", respectively, are selected as the holographic images, which will be encoded in the surface patterned hologram and the internal patterned hologram. Then, their calculated binary holograms are multiplied with the corresponding patterns containing the zones of selected 2D pattern, which forms the patterned holograms encoding different holographic images.

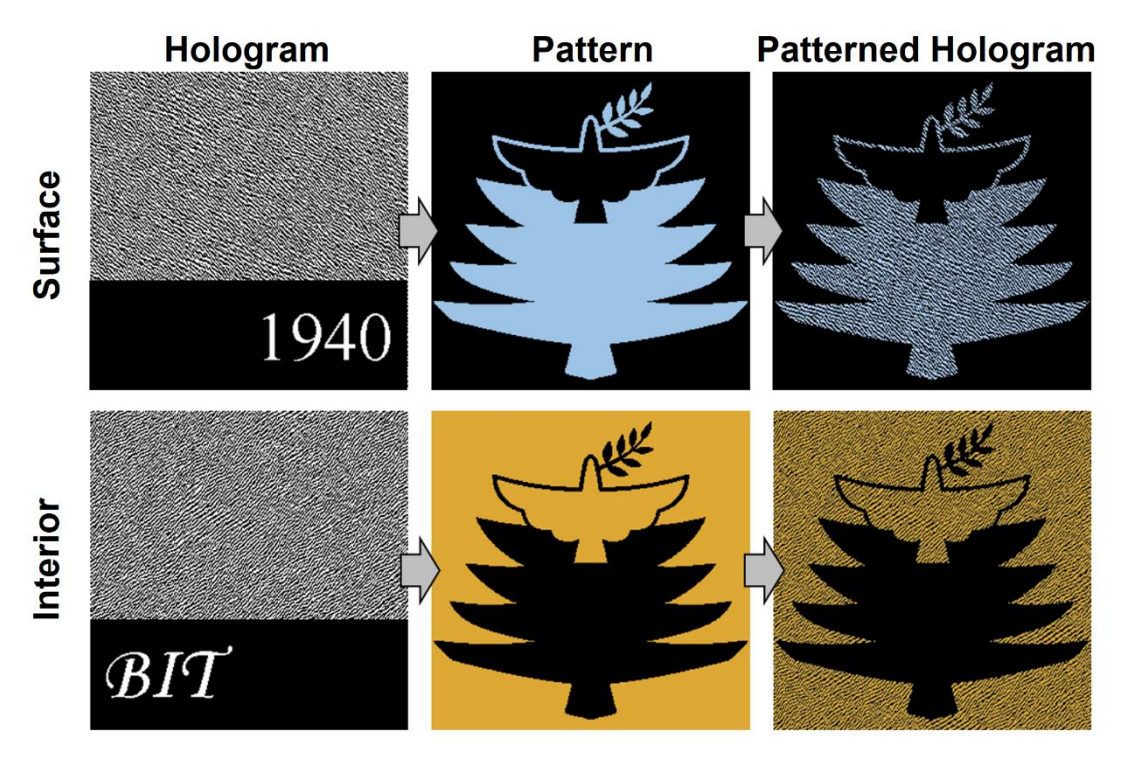


Figure S4. The design scheme of holographic patterns whose surface and interior patterned holograms encode different images

5. Influence of layer spacing on the holographic image

Holographic patterns with different layer spacing of 10, 20, 30, 40, 50 and 60 μ m were fabricated using dynamic 3D spatially modulated femtosecond pulses with same pulse energy. Their corresponding holographic images are shown in Figure S5 (a). With the increase of layer spacing, the intensity of image "1940" corresponding to the surface patterned hologram remained nearly constant, while the intensity of image "BIT" corresponding to the interior patterned hologram decreased slightly. In order to quantitatively compare the intensity changes, the average intensity I_{mean1} and I_{mean2} of optical spots contained in the image "BIT" and "1940" were calculated, and the variation curve of the intensity ratio under different layer spacing was drawn in Figure S5 (b). When the layer spacing was less than 50 μ m, there was little change in the intensity ratio of the two images. But the intensity ratio began to decrease when the layer spacing was greater than 50 μ m, meaning the intensity reduce of image "BIT" in the holographic image.

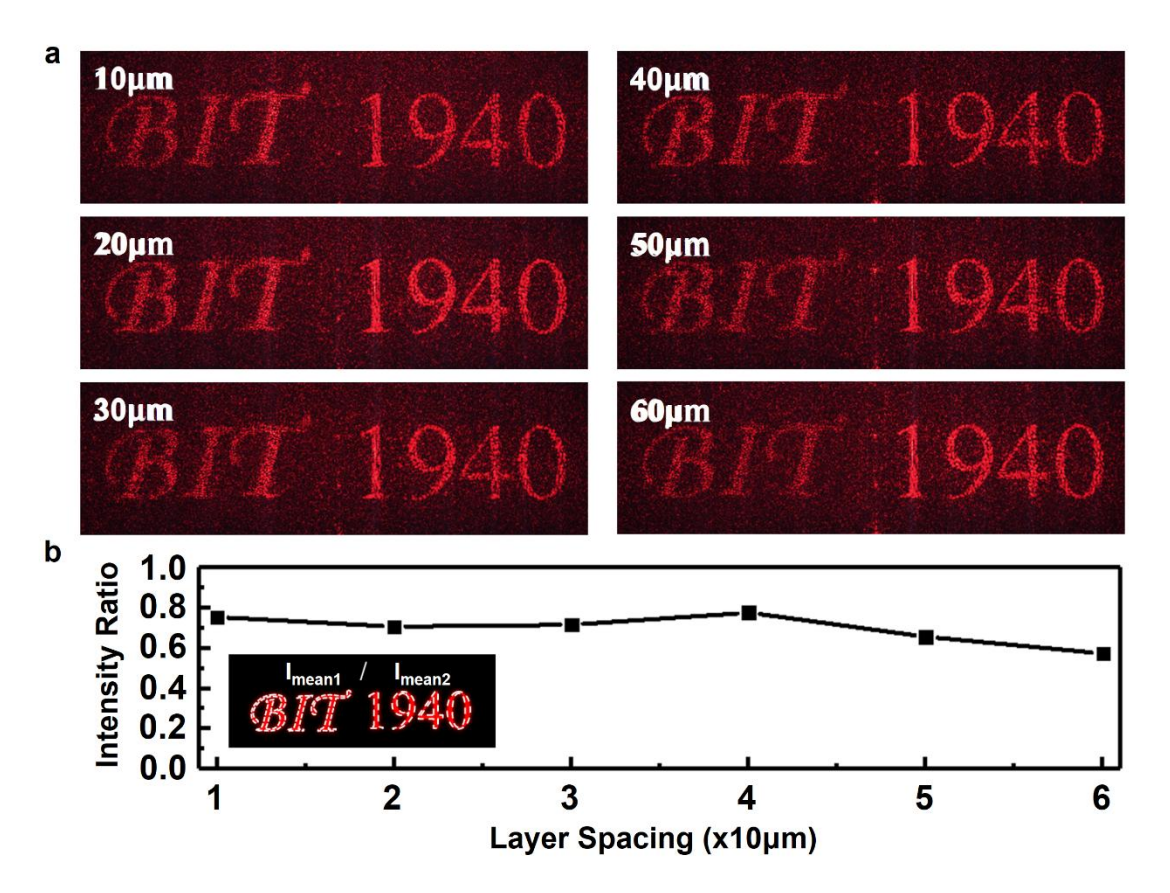


Figure S5. (a) Reconstructed holographic images of holographic patterns with different layer spacings. (b) Variation of the average intensity ratio of the image "BIT" to "1940" with the increase of layer spacing.

6. 3D morphological characterization of surface structures after ultrasonic treatment

The 3D morphology of the surface structures after ultrasonic treatment was measured by using atomic force microscope. From the result shown in Figure S6 (a), it can be found that the microholes transformed into microcraters with smooth inner surface. Moreover, the cross-section profile depicted in Figure S6 (b) also indicates that the depth of structure was reduced, compared with the longitudinal section of the microhole shown in Figure 3 (a). Therefore, instead of cleaning up the debris attached on the inner surface of microholes, the ultrasonic treatment changed the original microholes with rough surface into microcraters with smooth surface.

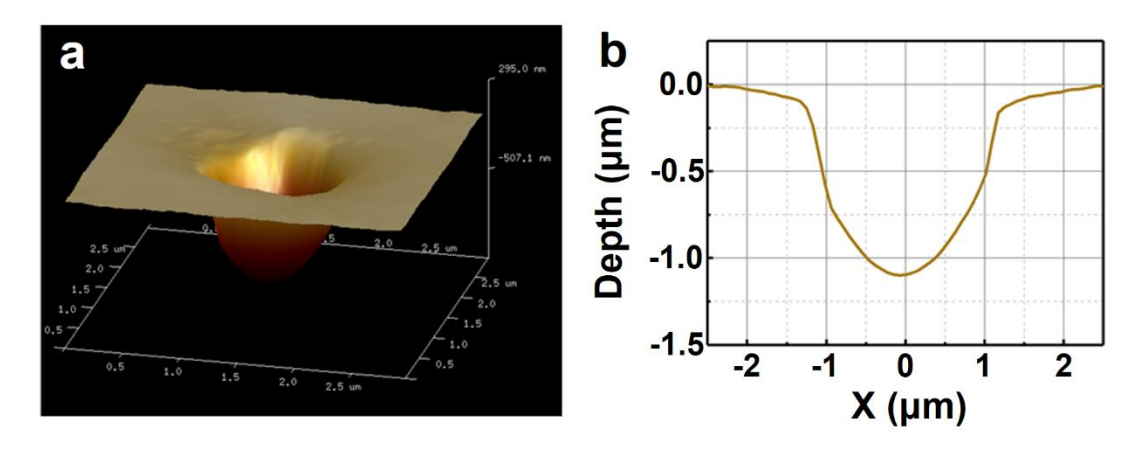


Figure S5. (a) The 3D morphology of microcrater characterized by atomic force microscope. (b) The corresponding cross-section profile plotted along the center of 3D morphology.

7. Optical transmittance comparison between microholes and microcraters

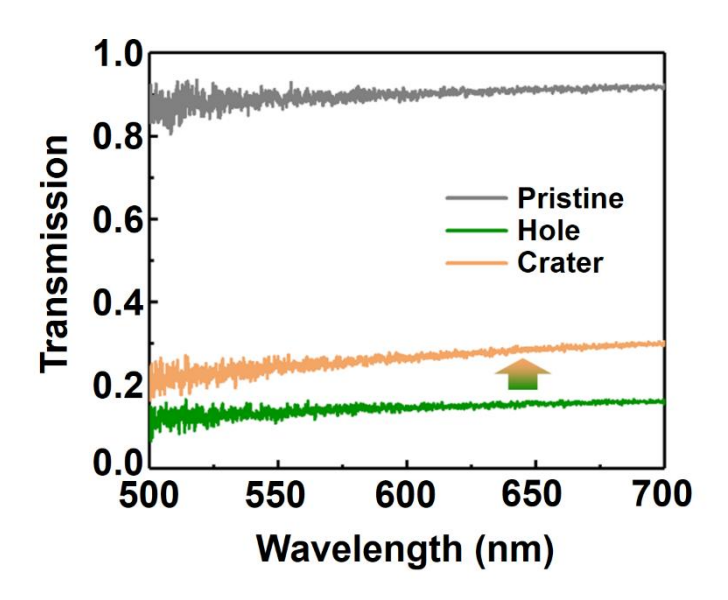


Figure S7. Optical transmittance spectra of the pristine PMMA, microhole array and microcrater array in the visible spectrum.